

# Saturable and two-photon absorption in zinc nanoparticles photodeposited onto the core of an optical fiber

P. Zaca-Morán,<sup>1,\*</sup> R. Ramos-García,<sup>2</sup> J. G. Ortega-Mendoza,<sup>3</sup> F. Chávez,<sup>1</sup>  
G. F. Pérez-Sánchez,<sup>1</sup> and C. Felipe<sup>4</sup>

<sup>1</sup>Instituto de Ciencias, Universidad Autónoma de Puebla, CP 72050, Puebla, Pue., Mexico

<sup>2</sup>Departamento de Óptica, Instituto Nacional de Óptica y Electrónica, CP 72840, Tonantzintla, Pue., Mexico

<sup>3</sup>División de Ingenierías, Universidad Politécnica de Tulancingo, CP 43629, Hidalgo, Mexico

<sup>4</sup>Departamento de Biociencias e Ingeniería, CIEMAD, Instituto Politécnico Nacional, CP 07340, D. F., Mexico

\*[zmoran\\_placido@yahoo.com.mx](mailto:zmoran_placido@yahoo.com.mx)

**Abstract:** In this work, the simultaneous presence of saturable (SA) and two-photon absorption (TPA) in zinc nanoparticles (ZnNPs) photodeposited onto the core of an optical fiber was studied in the nanosecond regime with the P-scan method using a high gain pulsed erbium-doped fiber amplifier. An analysis based on Mie theory was carried out to demonstrate the influence of the absorption coefficient with the particles sizes in the proximity of surface plasmon resonance (SPR). The shift from TPA to SA has been observed as the irradiance is increased. It was found that for irradiances lower than 5 MW/cm<sup>2</sup>, TPA is dominant, whereas for irradiances higher than 5 MW/cm<sup>2</sup>, the SA becomes dominant. Furthermore, the values of the nonlinear absorption coefficient and the imaginary part of third-order nonlinear optical susceptibility were calculated numerically from the transmittance measured. Such TPA makes ZnNPs a candidate for optical limiting applications, and SA makes them a candidate for applications in pulsed fiber laser systems.

©2015 Optical Society of America

**OCIS codes:** (060.2390) Fiber optics, infrared; (160.4236) Nanomaterials; (230.4320) Nonlinear optical devices; (240.6680) Surface plasmons.

---

## References and links

1. G. S. He, W.-C. Law, A. Baev, S. Liu, M. T. Swihart, and P. N. Prasad, "Nonlinear optical absorption and stimulated Mie scattering in metallic nanoparticle suspensions," *J. Chem. Phys.* **138**(2), 024202 (2013).
2. M. Halonen, A. A. Lipovskii, and Y. P. Svirko, "Femtosecond absorption dynamics in glass-metal nanocomposites," *Opt. Express* **15**(11), 6840–6845 (2007).
3. R. A. Ganeev, M. Suzuki, M. Baba, M. Ichihara, and H. Kuroda, "Low- and high-order nonlinear optical properties of Au, Pt, Pd, and Ru nanoparticles," *J. Appl. Phys.* **103**(6), 063102 (2008).
4. P. Zaca-Morán, E. Kuzin, J. Torres-Turiján, J. G. Ortega-Mendoza, F. Chávez, G. F. Pérez-Sánchez, and L. C. Gómez-Pavón, "High gain pulsed erbium-doped fiber amplifier for the nonlinear characterization of SWCNTs photodeposited on optical fibers," *Opt. Laser Technol.* **52**, 15–20 (2013).
5. J. Gupta, C. Vijayan, S. K. Maurya, and D. Goswami, "Efficient ultrafast optical limiting using single walled carbon nanotubes functionalized noncovalently with free base and metalloporphyrins," *J. Appl. Phys.* **109**(11), 113101 (2011).
6. G. X. Chen and M. H. Hong, "Time-resolved analysis of nonlinear optical limiting for laser synthesized carbon nanoparticles," *Appl. Phys., A Mater. Sci. Process.* **101**(3), 467–470 (2010).
7. N. V. Kamanina, A. I. Plekhanov, S. V. Serov, V. P. Savinov, P. Shalin, and F. Kajzar, "Correlation between photoconductive and nonlinear optical characteristics of fullerene- and nanotubes-doped organic composites," *Nonlinear Opt., Quantum Opt.* **40**(1), 307–377 (2010).
8. N. V. Kamanina, S. V. Serov, and V. P. Savinov, "Photorefractive properties of nanostructured organic materials doped with fullerenes and carbon nanotubes," *Tech. Phys. Lett.* **36**(1), 40–42 (2010).
9. E. F. Sheka, B. S. Razbirin, A. N. Starukhin, D. K. Nelson, M. Yu. Degunov, R. N. Lyubovskaya, and P. A. Troshin, "The nature of enhanced linear and nonlinear optical effects in fullerene solutions," *J. Exp. Theor. Phys.* **108**(5), 738–750 (2009).

10. M.-S. Hu, H.-L. Chen, C.-H. Shen, L.-S. Hong, B.-R. Huang, K.-H. Chen, and L.-C. Chen, "Photosensitive gold-nanoparticle-embedded dielectric nanowires," *Nat. Mater.* **5**(2), 102–106 (2006).
11. A. M. Malyarevich, K. V. Yumashev, and A. A. Lipovskii, "Semiconductor-doped glass saturable absorbers for near-infrared solid state lasers," *J. Appl. Phys.* **103**(8), 081301 (2008).
12. D. K. Mynbaev and V. Sukharenko, "Plasmonic-based devices for optical communications," *Int. J. High Speed Electron. Syst.* **21**(1), 1250006 (2012).
13. Q. Liu, X. He, X. Zhao, F. Ren, X. Xiao, C. Jiang, X. Zhou, L. Lu, H. Zhou, S. Qian, B. Poumellec, and M. Lancry, "Enhancement of third-order nonlinearity in Ag-nanoparticles-contained chalcogenide glasses," *J. Nanopart. Res.* **13**(9), 3693–3697 (2011).
14. C. Torres-Torres, J. A. Reyes-Esqueda, J. C. Cheang-Wong, A. Crespo-Sosa, L. Rodríguez-Fernández, and A. Oliver, "Optical third-order nonlinearity by nanosecond and picosecond pulses in Cu nanoparticles in ion-implanted silica," *J. Appl. Phys.* **104**(1), 014306 (2008).
15. G. Ma, J. He, S.-H. Tang, W. Sun, and Z. Shen, "Size-dependence of nonlinearity in metal: Dielectric composite system induced by local field enhancement," *J. Nonlinear Opt. Phys. Mater.* **12**(2), 149–155 (2003).
16. T. Klar, M. Perner, S. Grosse, G. von Plessen, W. Spirkel, and J. Feldmann, "Surface-plasmon resonances in single metallic nanoparticles," *Phys. Rev. Lett.* **80**(19), 4249–4252 (1998).
17. E. Hutter and J. H. Fendler, "Exploitation of localized surface plasmon resonance," *Adv. Mater.* **16**(19), 1685–1706 (2004).
18. S. Zhu and W. Zhou, "Optical properties and immunoassay applications of noble metal nanoparticles," *J. Nanomater.* **2010**, 1–12 (2010).
19. H. Amekura, N. Umeda, K. Kono, Y. Takeda, N. Kishimoto, Ch. Buchal, and S. Mantl, "Dual surface plasmon resonances in Zn nanoparticles in SiO<sub>2</sub>: an experimental study based on optical absorption and thermal stability," *Nanotechnology* **18**(39), 395707 (2007).
20. J. G. Ortega-Mendoza, F. Chávez, P. Zaca-Morán, C. Felipe, G. F. Pérez-Sánchez, G. Beltran-Pérez, O. Goiz, and R. Ramos-García, "Selective photodeposition of zinc nanoparticles on the core of a single-mode optical fiber," *Opt. Express* **21**(5), 6509–6518 (2013).
21. I. Calizo, K. A. Alim, V. A. Fonoberov, S. Krishnakumar, M. Shamsa, A. A. Balandin, and R. Kurtz, "Micro-Raman spectroscopic characterization of ZnO quantum dots, nanocrystals and nanowires," *Proc. SPIE* **6481**, 64810N (2007).
22. J. Zhu, J.-J. Li, and J.-W. Zhao, "Tuning the wavelength drift between resonance light absorption and scattering of plasmonic nanoparticle," *Appl. Phys. Lett.* **99**(10), 101901 (2011).
23. C. F. Bohren and D. R. Huffman, *Absorption and Scattering of Light by Small Particles* (Wiley, 1983), Chap. 4.
24. M. P. Silverman, *Waves and Grains* (Princeton, 1998), Chap. 13.
25. R. Rangel-Rojo, S. Yamada, H. Matsuda, H. Kasai, H. Nakanishi, A. K. Kar, and B. S. Wherrett, "Spectrally resolved third-order nonlinearities in polydiacetylene microcrystals: influence of particle size," *J. Opt. Soc. Am. B* **15**(12), 2937–2945 (1998).
26. M. Hari, S. Mathew, B. Nithyaja, S. A. Joseph, V. P. N. Nampoori, and P. Radhakrishnan, "Saturable and reverse saturable absorption in aqueous silver nanoparticles at off-resonant wavelength," *Opt. Quantum Electron.* **43**(7), 43–49 (2012).
27. L. Irimpan, A. Deepthy, B. Krishnan, V. P. N. Nampoori, and P. Radhakrishnan, "Nonlinear optical characteristics of self-assembled films of ZnO," *Appl. Phys. B* **90**(3–4), 547–556 (2008).
28. J. Zheng, C. Zhou, M. Yu, and J. Liu, "Different sized luminescent gold nanoparticles," *Nanoscale* **4**(14), 4073–4083 (2012).
29. R. Kuladeep, L. Jyothi, P. Prakash, S. M. Shekhar, M. D. Prasad, and D. N. Rao, "Investigation of optical limiting properties of Aluminium nanoparticles prepared by pulsed laser ablation in different carrier media," *J. Appl. Phys.* **114**(24), 243101 (2013).
30. G. Fan, S. Qu, Q. Wang, C. Zhao, L. Zhang, and Z. Li, "Pd nanoparticles formation by femtosecond laser irradiation and the nonlinear optical properties at 532 nm using nanosecond laser pulses," *J. Appl. Phys.* **109**(2), 023102 (2011).
31. Y. H. Lee, Y. Yan, L. Polavarapu, and Q.-H. Xu, "Nonlinear optical switching behavior of Au nanocubes and nano-octahedra investigated by femtosecond Z-scan measurements," *Appl. Phys. Lett.* **95**(2), 023105 (2009).
32. H. Morkoc and U. Ozgur, *Zinc Oxide, Fundamentals, Materials and Device Technology* (Wiley, 2007), Chap. 3.

## 1. Introduction

Considerable research has been done on nonlinear optical properties of nanostructured materials as a new class of optical limiters or optical absorbers. These properties have been widely explored in noble metals [1–3], carbon nanostructures [4–6], and fullerenes [7–9], for applications in high-capacity communications, ultrafast switching, signal regeneration, and high speed demultiplexing [10–12] among others.

Nowadays, the nonlinear optical properties of metal nanoparticles have attracted great interest due to its high optical Kerr effect ( $\chi^{(3)}$ ). These properties of metal nanoparticles are mainly based on their resonance frequency excited by electromagnetic fields, phenomenon

known as surface plasmon [12–16]. Surface plasmons are described as collective oscillations of the conduction-band electrons on the surface of continuous thin metallic films, gratings, nanohole arrays, or on confined nanostructures such as nanopillars, nanorods or nanospheres [15–17]. When the nanostructures are confined, surface plasmons are known as localized surface plasmons (LSPs) whose excitation is due to the radiation of certain wavelengths. The degree of excitation is quantified by their extinction coefficients. These coefficients result from the contribution of scattering and absorption bands of light whose solution is given by the Mie theory [18, 19].

In this work, the nonlinear absorption properties of zinc nanoparticles (ZnNPs) photodeposited onto the core of an optical fiber were studied using a high gain pulsed amplifier. The size-dependent absorption of ZnNPs was analyzed in the proximity of surface plasmon resonance (SPR) in the infrared region. Besides, the nonlinear absorption coefficient and the value of the imaginary part of the third-order nonlinear optical susceptibility were obtained by P-scan technique. To the best of our knowledge, the intensity-dependent switching of two-photon absorption (TPA) and saturable absorption (SA) as not been reported before in ZnNPs. The relevance of the nonlinear optical properties of ZnNPs deposited onto the core of an optical fiber may result in cheap and efficient optical devices.

## 2. Experiment

In our experiment, ZnNPs were photodeposited following the procedure previously reported [20]. Here, we showed laser-induced deposition of nanoparticles due to an interplay of convective fluid flow due to the heat transfer from ZnNPs to the solution and optical forces. The absorption and scattering forces partially compensate the Stokes force for certain particle size on the vicinity of fiber end allowing the photodeposition of nanoparticles. Firstly, 10 mg of zinc powder in 10 ml of isopropyl alcohol were mixed and homogenized using an ultrasonic bath for more than 20 minutes. Later, an optical fiber SMF-28 was prepared by removing the coating, cleaving it and placing it inside the solution as shown in Fig. 1. Finally, we used a continuous wave fiber laser ( $\lambda = 1550$  nm) to carry out the photodeposition process, as well as a power meter to measure the transmission.

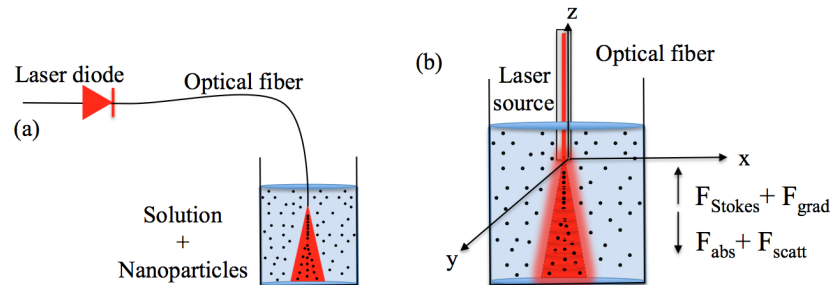


Fig. 1. (a) Experimental setup for the photodeposition of ZnNPs onto an optical fiber end (b) Representation of the model where the light is propagating along -z axis. The scattering and absorption forces are directed along the -z axis and Stokes and gradient forces are directed along the z axis.

Figure 2(a) shows a scanning electron microscope (SEM) image of ZnNPs photodeposited onto the core of an optical fiber. In the same figure, some particles were also deposited on the fiber cladding. Because of the limited resolution of our SEM, we could not determine actual size of the nanoparticles deposited. According to our previous work [20], the size and amount of ZnNPs deposited onto the core depend on the beam properties and the immersion time. Under these conditions, we can consider that the sizes of nanoparticles deposited onto the core of the optical fiber are smaller than 100 nm of radii with a thickness of 500 nm approximately.

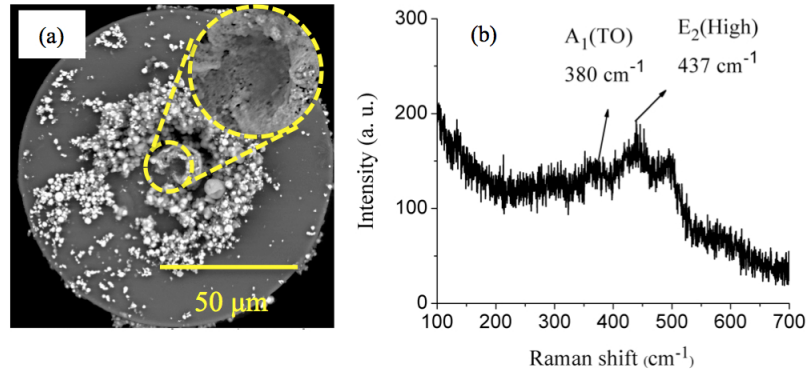


Fig. 2. (a) SEM image of the ZnNPs deposited on the core of an optical fiber, the circle is a closer view of the core. (b) Micro-Raman spectrum recorded on the core region of the optical fiber at room-temperature.

Figure 2(b) shows the micro-Raman spectrum measured onto the core of the optical fiber. The spectrum shows two weak peaks around  $380$  and  $437\text{ cm}^{-1}$ , which are associated with the active transversal optical component  $A_1(\text{TO})$  and Raman-active optical phonon mode  $E_2(\text{High})$ , respectively. These peaks correspond to the ZnO wurtzite hexagonal phase [21]. No additional peaks in the remainder spectrum were identified. The low-intensity peaks of the Raman spectrum indicate that the contribution of ZnO onto the fiber core is minimal; this should be meaning that these nanoparticles are formed mainly of zinc metal. This situation is an expected result, since; it is well-known that in opaque materials such as metal and narrow band-gap semiconductors are non-Raman active materials. The result is in good agreement with the x-ray previously reported [20].

The absorption properties of the ZnNPs deposited onto the fiber core were studied by irradiance dependent transmission measurements using a high gain pulsed erbium-doped fiber amplifier previously reported [4]. It consists of an optical signal at  $1550\text{ nm}$  emitted by a distributed feedback laser which is amplified by two identical stages in reflective configuration using one fiber Bragg grating (FBG) in every stage. The experimental results show that using  $1\text{ kHz}$  of frequency and  $10\text{ ns}$  of temporal pulse duration, it is possible to obtain up to  $1000\text{ W}$  output peak power. This high gain amplifier can be used to carry out the absorption characterization of any kind of nanomaterials deposited onto optical fibers by means of the Power-scan or P-scan technique [4]. The P-scan technique works similarly as the Z-scan technique, but instead of varying the applied intensity by changing the beam spot size, the intensity is changed and the sample transmission is measured. This technique offers the advantage of being faster to measure than Z-scan, in addition it is less sensitive to reflections losses.

### 3. Theoretical calculations

Collective motion of free electrons confined in the metal nanoparticles photodeposited on the core of an optical fiber gives rise to the LSPs and a strong nonlinear optical response, whose excitation is quantified by their extinction coefficient. This coefficient results from the contribution of scattering and absorption bands [16].

The classical Mie theory can be used to understand the absorption spectra of a nanoparticle. This theory assumes that a particle and the surrounding medium are homogeneous and can be described by bulk optical dielectric functions. Solving Maxwell's equations lead the study of the relationship for the extinction cross-section,  $\sigma_{\text{ext}} (\sigma_{\text{ext}} = \sigma_{\text{abs}} + \sigma_{\text{sca}} = \text{absorption cross-section} + \text{scattering cross-section})$  for metallic nanoparticles as a summation over all electric and magnetic oscillations [22].

To evaluate the optical response of the ZnNPs deposited onto the fiber, we applied the Mie theory. By solving Maxwell's equations, Mie derived an analytical solution for the extinction, scattering, and absorption cross sections of a metal sphere embedded in a homogeneous medium by [23, 24]

$$C_{\text{ext}} = \frac{2\pi r^2}{x^2} \sum_{l=1}^{\infty} (2l+1) \text{Re}(a_l + b_l), \quad (1)$$

$$C_{\text{sca}} = \frac{2\pi r^2}{x^2} \sum_{l=1}^{\infty} (2l+1) (|a_l|^2 + |b_l|^2), \quad (2)$$

$$C_{\text{abs}} = C_{\text{ext}} - C_{\text{sca}}, \quad (3)$$

where  $l$  denotes the multipole order of the excited particle plasmons,  $x = 2\pi r / \lambda$  represents a size parameter proportional to the ratio of the sphere radius  $r$  to wavelength  $\lambda$ ; for a wavelength of 1550 nm, and spheres with radii  $\geq 100$  nm,  $x \sim 0.4$ . The Mie coefficients are

$$a_l = \frac{m\psi_l(mx)\psi_l'(x) - \psi_l(x)\psi_l'(mx)}{m\psi_l(mx)\xi_l'(x) - \xi_l(x)\psi_l'(mx)}, \quad (4)$$

$$b_l = \frac{\psi_l(mx)\psi_l'(x) - m\psi_l(x)\psi_l'(mx)}{\psi_l(mx)\xi_l'(x) - m\xi_l(x)\psi_l'(mx)}, \quad (5)$$

expressed by Ricatti-Bessel functions  $\psi_l$  and  $\xi_l$ , contain the dependence on the material specific complex dielectric functions through  $m^2 = \epsilon_{\text{metal}} / \epsilon_{\text{medium}}$ .

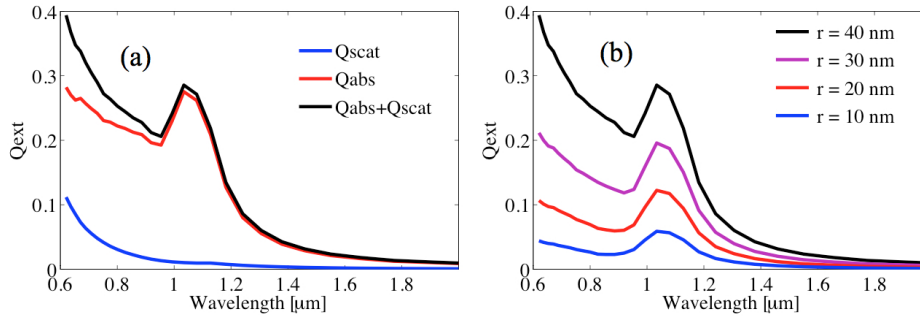


Fig. 3. Dependence of the extinction for zinc spheres: (a) scattering and absorption are separated for  $r = 40$  nm, and (b) comparative extinction for  $r < 40$  nm.

The spectral dependence of the real and imaginary part of the complex refractive indices to Zn was obtained from [19]. In these studies the authors show that the nanoparticles have two absorption peaks at 1.2 and 4.8 eV corresponding to 1032 nm, and 326 nm respectively. Using the optical properties of ZnNPs previously reported, we carried out the study of light scattering and absorption from small metal particles deposited on the core of an optical fiber in the proximity of surface plasmon resonance of 1.2 eV. The calculations show that for zinc spheres smaller than 100 nm of radius, the absorption dominates over scattering, and determines the extinction coefficient (Fig. 3). On the other hand, for radii larger than 100 nm, the scattering dominates over absorption and determines the extinction coefficient (Fig. 4).

According to the obtained results, we believe that those plasmonic excitations in the proximity of SPR to 1032 nm are the responsible for the nonlinear optical response in the ZnNPs deposited onto the core of the optical fiber. Accordingly, much attention was given to

characterize nonlinear absorption of metal nanoparticles by relevant methods where the irradiance dependence of refractive index and absorption are manifested as transmission variation of the material such as the Z-scan or P-scan technique [7].

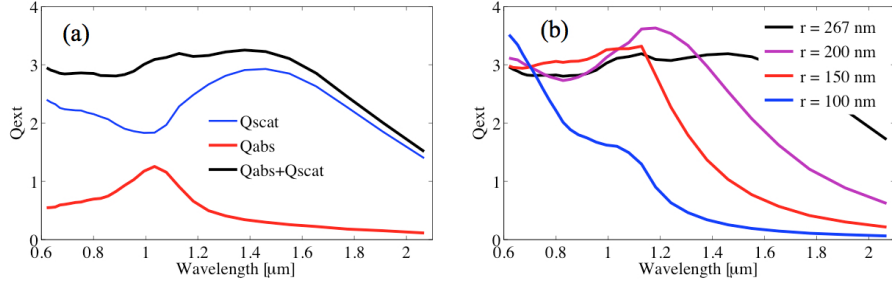


Fig. 4. Dependence of the extinction for zinc spheres: (a) scattering and absorption are separated for  $r = 256$  nm, and (b) comparative extinction for  $r > 100$  nm.

In this work, the presence of TPA and SA absorption mechanisms are present simultaneously and operate in two different intensity regions. Previous results had showed that metallic nanoparticles with size in the nanometer range exhibit intensity-dependent absorption described by the linear and nonlinear absorption coefficients  $\alpha(I) = \alpha_0 + \alpha_2 I + \alpha_4 I^2 \dots$ , where  $\alpha_0$  is the linear absorption coefficient ( $\text{cm}^{-1}$ ),  $\alpha_n$  is the nonlinear absorption coefficient with order  $(n + 1)$ th, and  $I$  is the irradiance. For small nonlinear effects, the optical absorption coefficient can be reduced to the first two terms. Here, we have to consider the transmittance of the fiber with ZnNPs under two situations: (1) in the presence of TPA ( $0.44\text{-}5 \text{ MW/cm}^2$ ) and (2) in the presence of SA ( $5\text{-}100 \text{ MW/cm}^2$ ).

In presence of TPA, the optical nonlinearity is expressed by [24, 25]

$$\alpha(I) = \alpha_0(I) + \beta_{TPA} I, \quad (6)$$

where  $\beta_{TPA}$  is the nonlinear absorption cross section ( $\text{cmW}^{-1}$ ). Since  $\beta_{TPA} I \ll \alpha_0(I)$ , under low irradiance conditions the absorption coefficient is given by  $\alpha(I) \approx \alpha_0(I)$ .

When SA is presented, Eq. (6) can be changed to

$$\alpha(I) = \frac{\alpha_0}{1 + I/I_{sat}}, \quad (7)$$

where  $I_{sat}$  is the saturation intensity defined as the intensity where the change in the transmittance has reached 50% of its modulation depth. The nonlinear absorption, for low excitation radiation, can calculate by considering the  $I/I_{sat} \ll 1$  limit to Eq. (7),  $\alpha(I) \approx \alpha_0 - (\alpha_0 / I_{sat}) I$ , and by comparison with 1,  $\beta_{SA} \approx -\alpha_0 / I_{sat}$ .

The transmittance curve can be expressed as a function of the irradiance by applying Beer-Lambert law equation given by

$$T = e^{-\alpha(I)L}, \quad (8)$$

where  $L$  is the sample thickness. By substituting Eq. (6) or Eq. (7) into Eq. (8), we can obtain the transmittance in presence of TPA or SA, respectively.

We can use Eqs. (6)-(8) to fit the experimental data of P-scan trace, and  $\beta$  can be treated as an adjustable parameter. From the value of  $\beta$ , we can calculate the imaginary part of

susceptibility  $Im(\chi^{(3)})$  through the following expression in the international system (SI) of units:

$$Im(\chi^{(3)}) = \frac{\lambda \epsilon_0 n_0^2 c \beta}{4\pi}, \quad (9)$$

where  $n_0$  is the linear refractive index of the ZnNPs ( $n_0 \approx 1.3$  for zinc [19]),  $\epsilon_0$  is the permittivity of free space ( $8.85 \times 10^{-12}$  (F/m)) and  $c$  is the velocity of light in vacuum. The expression (9) gives units of ( $m^2 / V^2$ ). We can convert the units of  $Im(\chi^{(3)})$  in (*esu*) using the conversion formula  $1 (m^2 V^{-2}) = 9 \times 10^8 (esu)$ .

#### 4. Results and discussions

To study the nonlinear absorption response of the ZnNPs photodeposited onto optical fibers, we used the P-scan technique with samples of 3 dB of transmission under the same conditions at 1550 nm. Each experimental point represents fifty-pulse average and the intensity was kept as low as possible to avoid the detaching of ZnNPs in the fiber due to radiation pressure. Figure 5 shows the dependence of the transmittance obtained from the ZnNPs deposited on the core of an optical fiber as function of the applied irradiance. According to the results obtained, the transmittance begins with a maximum value, which decreases rapidly to lower intensities value. Once the minimum value is reached, the transmittance increases until it saturates. It was verified that no transmission variations for an empty sample, without nanoparticles in the core, in the P-scan measurement.

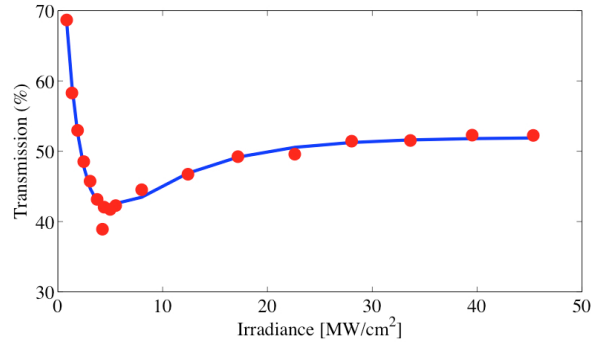


Fig. 5. Dependence of the transmittance of ZnNPs deposited on the core of an optical fiber.

In order to calculate the values of nonlinear absorption coefficient and the imaginary part of the third-order susceptibility for TPA and SA, the results obtained in Fig. 5 were divided in two parts as follows. Figure 6(a) shows a large decrease in transmittance with increasing irradiance to irradiances lower than  $5 \text{ MW/cm}^2$ . This nonlinear behavior is a typical characteristic of optical limiting phenomenon. The value of the imaginary part of third-order susceptibility was calculated according to the curve fitting and using Eq. (9), obtaining  $\beta_{TPA} \approx 3.56 \times 10^{-5} (m/W)$  and  $Im(\chi^{(3)}) \approx 1.97 \times 10^{-14} (m^2/V^2)$  ( $\approx 1.75 \times 10^{-5} esu$ ), respectively. Figure 6(b) shows an increase in transmittance with increasing irradiance higher than  $5 \text{ MW/cm}^2$ . This nonlinear behavior is a typical characteristic for SA phenomenon. The value of the imaginary part of third-order susceptibility was calculated according to the curve fitting to obtain  $\beta_{SA} \approx -2.38 \times 10^{-6} (m/W)$  and  $Im(\chi^{(3)}) \approx -1.31 \times 10^{-15} (m^2/V^2)$  ( $\approx -1.18 \times 10^{-6} esu$ ), respectively. According to the results, it is clearly illustrated that the nonlinear behavior from TPA to SA is intensity dependent. The changes observed in our experiments were fully reversible and reproducible. The measurements were repeated several

times to ensure reproducibility under the same conditions, which means no heating effects that transform the ZnNPs to zinc oxide nanoparticles.

There are several mechanisms that can give rise to the TPA attributed mainly to the absorption from free carriers, such as photoejection of electrons, nonlinear scattering, accumulative effect of excited state absorption (ESA), etc [26, 27]. However, it is well known that the metallic nanoparticles can absorb photons of visible and infrared spectrum, but only the electrons in the energy band adjacent to the Fermi level or the outmost electrons in the conduction band are involved in the recombination process through interband or intraband transitions [28].

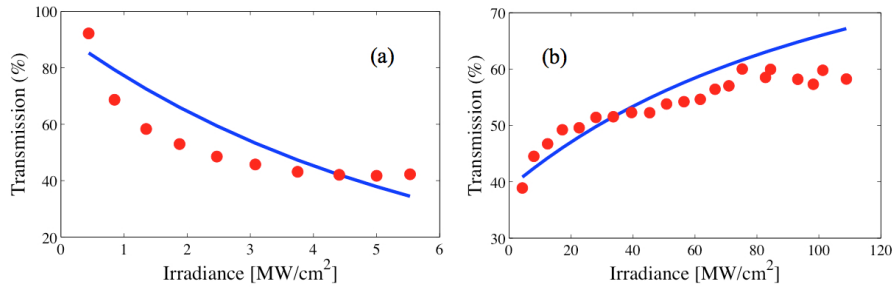


Fig. 6. Dependence of the transmittance as a function of the irradiance to ZnNP, a) Irradiance less to 5 MW/cm<sup>2</sup>, b) irradiance less to 70 MW/cm<sup>2</sup>.

When the absorption process is repeated, the photons can be excited again to a higher excited band; this process corresponds to TPA. We think that the result obtained in our experiments using low intensities at about 0.44-5 MW/cm<sup>2</sup> can be associated with the TPA process, because the absorption bands of the ZnNPs can be extended from the visible to near infrared region, which is associated with the size of the nanoparticle and the radiation source as it was showed before in Figs. 3 and 4. However we do not discard the possibility of finding other nonlinear behaviors such as the SA effects below to 0.44 MW/cm<sup>2</sup> because in our experiment of photodeposition was carried out at low-power with a transmission of 3 dB; this means  $T = 50\%$ . Particularly, if a laser source of 1550 nm is used to carry out nonlinear characterization in ZnNPs lower than 100 nm of radii, the infrared band (1032 nm) can be extended to the near infrared region, which is the requirement to TPA. The possibility of TPA caused by interband transition of photoexcited electrons was previously demonstrated in aluminum [29], palladium [30] and gold [31] nanoparticles.

Moreover, when we use moderate intensities in the experimental setup, the effects of the light pulses can result in the hot electrons mechanism or ground-state bleaching band, which have been a dominant contribution to nonlinear SA in metallic nanoparticles. Nowadays, some authors have reported that these hot electrons are the main responsible for the SA in plasmonic nanostructures and their thermal effects could change the properties of nanoclusters by saturated optical absorption, these thermal effects make transmission more transparent [14, 32].

Because the results of this work were performed in proximity of the zinc plasmon resonance in the nanosecond regime, we can conclude that a thermal effect is the most likely reason for the observed SA. That is, the thermal nonlinearities of the hot electrons in ZnNPs can be caused by the absorption properties in particles smaller than 100 nm of radii, as it is shown in Fig. 7. The figure shows that for particles smaller with radii <100 nm, the absorption is predominant and to particles with radii bigger than 100 nm, the scattering is predominant. As a result, the conduction band of ZnNPs smaller than 100 nm absorbs an important part of the incident energy. However, we do not discard the contribution of the effects due to the influence of the plasmon oscillation in the conduction band attributed to the ground-state bleaching band caused by intraband electron excitation. That is, ZnNPs can

behave as SA owing to the bleaching of the ground state plasmon band, which results in a transmittance increase. As the ground state is bleached, the system becomes increasingly transparent to the incident laser pulse at 1550 nm resulting in a saturation of absorption.

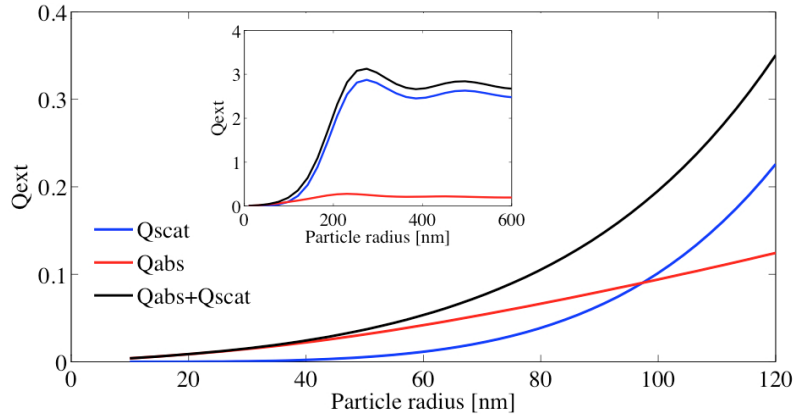


Fig. 7. Dependence of the extinction as a function of the particle radius.

Although the present study does not take into account the dependence of the pulse frequency or bleaching relaxation time, the nonlinear absorption coefficient is substantially high compared to the previous results carried out with others noble metal nanoparticles including those based on metal oxides thin films doped with various elements [13, 14, 32]. The improvement of this nonlinear absorption parameter is of significance from the point of view of efficient SA and versatile to applications in nonlinear optics and photonics.

Thus, the nonlinear absorption coefficients, measured by P-scan technique in the nanosecond regime reveals that the ZnNPs photodeposited onto the core of an optical fiber investigated in the present study have good nonlinear optical response and could be chosen as a good candidate with potential applications in optical communications, particularly in the near infrared region. To our knowledge, this is the first report of nonlinear characterization in the near infrared region of metallic nanoparticles deposited on the core of an optical fiber, which is ideal to make photonic devices for optical communications.

## 5. Conclusions

The study of nonlinear absorption of ZnNPs photodeposited onto the core of an optical fiber is presented. The nonlinear characterization was carried out using a gain high-pulsed amplifier in the nanosecond regime to 1550 nm by P-scan technique and the extinction properties of ZnNPs were studied using a numerical analysis based on Mie Theory in the proximity of SPR in the infrared region. Our analysis shows that the absorption dominates over scattering to particles smaller than 100 nm. With regards to the nonlinear characterization we found a change of sign from positive (TPA) at low irradiances to negative (SA) at high irradiances. Such TPA makes the ZnNPs a promissory candidate for optical limiting applications, and SA makes them a candidate for passive Q switching or mode locking in a laser cavity. This work opens a new scheme for the implementation of photonic devices, such as saturable absorbers for applications in pulsed fiber lasers systems or those based on optical fibers, besides this SA is easy and cheap to implement.

## Acknowledgments

This work was supported by CONACyT grant No. 130 983 and by Benemérita Universidad Autónoma de Puebla VIEP 2015 grant No. 00074.